




# The effects of chloride and sulphate on the growth of sulphide films on copper in anoxic sulphide solutions

Jian Chen<sup>1</sup>  | Xinran Pan<sup>1</sup> | Taylor Martino<sup>2</sup> | Christina Lilja<sup>3</sup>  |  
 Mehran Behazin<sup>4</sup> | Wilfred J. Binns<sup>4</sup> | Peter G. Keech<sup>4</sup>  | James J. Noël<sup>1,5</sup> |  
 David W. Shoemith<sup>1,5</sup>

<sup>1</sup>Department of Chemistry, University of Western Ontario, London, Ontario, Canada

<sup>2</sup>CanmetMATERIALS, Natural Resources Canada, Hamilton, Ontario, Canada

<sup>3</sup>Swedish Nuclear Fuel and Waste Management Company, Solna, Sweden

<sup>4</sup>Nuclear Waste Management Organization, Toronto, Ontario, Canada

<sup>5</sup>Surface Science Western, London, Ontario, Canada

## Correspondence

Jian Chen, Department of Chemistry, University of Western Ontario, London, ON N6A 5B7, Canada.

Email: [jchen496@uwo.ca](mailto:jchen496@uwo.ca)

## Funding information

Nuclear Waste Management Organization; Svensk

Kärnbränslehantering; Natural Sciences and Engineering Research Council of Canada

## Abstract

The corrosion of copper in chloride- and sulphate-containing solutions containing sulphide (ranging from  $5 \times 10^{-5}$  M to  $10^{-3}$  M) was studied by electrochemical impedance spectroscopy and the structure and physical properties of the copper sulphide deposits ( $\text{Cu}_2\text{S}$ ) were analysed by scanning electron microscopy. At low  $[\text{SH}^-]$ , a porous and non-protective deposit was formed, and the low corrosion rates were limited by sulphide transport, partially within the deposit and partially in the bulk of the solution. At higher  $[\text{SH}^-]$ , the corrosion rates were much higher and initially more rapid in chloride-containing than in sulphate-containing solutions, suggesting a direct role for chloride in the interfacial corrosion process. When the copper sulphide deposit thickened, the rate became limited by  $\text{Cu}^I$  transport within the more compact and more crystalline deposit formed. Changes in the morphology of the deposit suggest that chloride adsorption on the surfaces of the deposit inhibited the incorporation of  $\text{Cu}_3\text{S}_3$  clusters, transported from the corroding copper surface, into the growing crystals.

## KEYWORDS

copper, corrosion, nuclear waste disposal, sulphide

## 1 | INTRODUCTION

The universal approach for the permanent disposal of high-level nuclear waste (HLNW) is to bury it in a deep geological repository (DGR) with multiple barriers to provide safe containment and isolation.<sup>[1–3]</sup> In Sweden, Finland and Canada, the proposed container for the management and safe disposal of HLNW is either a cylindrical Cu shell containing a nodular cast iron insert (Sweden, Finland) or a Cu-coated carbon steel vessel

(Canada).<sup>[4–6]</sup> Within this sequence of barriers, comprising the geologic formation, compacted bentonite, container and spent fuel, the sealed waste container plays a vital role by providing the primary barrier against radionuclide release to the groundwater.<sup>[7]</sup> Although the initial exposure conditions within the DGR will be aerated and oxidising, the corrosion damage to Cu will be minor ( $<0.09$  mm<sup>[4,5,7]</sup>), since most of the entrained  $\text{O}_2$  trapped in the DGR upon sealing will be consumed rapidly by mineral and

This is an open access article under the terms of the Creative Commons Attribution License, which permits use, distribution and reproduction in any medium, provided the original work is properly cited.

© 2023 The Authors. *Materials and Corrosion* published by Wiley-VCH GmbH.

microbial reactions occurring in the bentonite clay compacted around the container or by the corrosion of structural steel within the DGR.<sup>[5]</sup> Once anaerobic conditions are established at the Cu container surface,<sup>[8,9]</sup> the long-term threat to container durability and integrity will be the degradation by reaction with sulphide ( $\text{SH}^-$ ), remotely produced by the activities of sulphate-reducing bacteria.<sup>[10–12]</sup>

Previous studies<sup>[12–27]</sup> showed that Cu would corrode rapidly in the presence of  $\text{SH}^-$ , leading to the deposition of chalcocite ( $\text{Cu}_2\text{S}$ )<sup>[13]</sup> on the Cu surface. The structure and properties of the  $\text{Cu}_2\text{S}$  film were shown to depend on the  $[\text{SH}^-]$ , the transport flux of  $\text{SH}^-$  to the corroding Cu surface, and the influence of other groundwater species (i.e.,  $\text{Cl}^-$ ,  $\text{SO}_4^{2-}$  and  $\text{HCO}_3^-/\text{CO}_3^{2-}$ ), which interfered with sulphide film formation by competition with  $\text{SH}^-$  for surface sites on the Cu surface.<sup>[26]</sup> This competition limited the formation of the chemisorbed  $\text{Cu}(\text{SH})_{\text{ads}}$ , which is the essential precursor for film formation. It has been shown that, under anodically polarised conditions,  $\text{Cu}_2\text{S}$  film growth in  $\text{SH}^-$  solutions with low ionic strength is controlled by ionic migration within pores in the film, while at high ionic strength, film growth is dependent on the  $[\text{SH}^-]$ . In solutions with high ionic strength but low  $[\text{SH}^-]$ ,  $\text{Cu}_2\text{S}$  film growth was limited by the rate of the interfacial anodic reaction to produce  $\text{Cu}(\text{SH})_{\text{ads}}$  at the base of pores in the film, and in solutions with high ionic strength and high  $[\text{SH}^-]$ ,  $\text{Cu}_2\text{S}$  film growth was limited by the transport of Cu species in a more compact film. The presence of  $\text{SO}_4^{2-}$  was found to suppress the growth of porous  $\text{Cu}_2\text{S}$  films to a greater extent than  $\text{Cl}^-$  does under these anodic conditions. It was suggested that this could be attributed to the strong co-adsorption of  $\text{SO}_4^{2-}$  and  $\text{H}_2\text{O}$  on the Cu surface.<sup>[26]</sup>

Long-term studies<sup>[13–15,17,18,20–23]</sup> have demonstrated that, under corrosion conditions, the structure and properties of the  $\text{Cu}_2\text{S}$  film vary greatly with the exposure conditions. When the bulk  $[\text{SH}^-]$  (i.e.,  $5 \times 10^{-5}$  M), the  $\text{SH}^-$  flux and the  $[\text{Cl}^-]$  (i.e., 0.1 M) were low, leading to even lower  $[\text{SH}^-]$  at the Cu surface, the  $\text{Cu}_2\text{S}$  film was very porous and nonprotective, and its growth was controlled by the flux of  $\text{SH}^-$  to the  $\text{Cu}_2\text{S}$  film/electrolyte interface. However, when the bulk  $[\text{SH}^-]$  was high (i.e.,  $\geq 5 \times 10^{-4}$  M), creating a higher  $\text{SH}^-$  flux at the Cu surface, and the  $[\text{Cl}^-]$  was low (i.e., 0.1 M), the  $\text{Cu}_2\text{S}$  film formed was compact and at least partially protective. Under these conditions, Cu corrosion was controlled by  $\text{Cu}^+$  diffusion in the  $\text{Cu}_2\text{S}$  film. With both high  $[\text{SH}^-]$  (i.e.,  $1 \times 10^{-3}$  M) and high  $[\text{Cl}^-]$  (i.e.,  $\geq 1.0$  M), the structure and properties of the  $\text{Cu}_2\text{S}$  film changed from compact to porous, with  $\text{Cl}^-$  interfering with film growth in a number of ways: (1) displacing adsorbed  $\text{SH}^-$  from the Cu surface to inhibit the first step in the overall

corrosion process; (2) inducing and maintaining the porosity in the  $\text{Cu}_2\text{S}$  film; and (3) facilitating the transport of Cu into the solution when the  $[\text{Cl}^-]$  was extremely high (i.e., 5.0 M).<sup>[20]</sup> However, when  $\text{SO}_4^{2-}$  was present rather than  $\text{Cl}^-$  in  $\text{SH}^-$  solutions, it was uncertain whether  $\text{SO}_4^{2-}$  exhibited an influence under corrosion conditions similar to that observed in electrochemical experiments.<sup>[26]</sup> In addition, there is a need to validate whether the rate-determining step for Cu canister corrosion under DGR conditions remains the same as that observed in a solution containing  $\text{Cl}^-$ .

In this study, we compared the corrosion potential ( $E_{\text{CORR}}$ ) and the electrochemical impedance spectroscopic (EIS) responses of Cu in anoxic  $\text{SH}^-$  solutions containing either  $\text{SO}_4^{2-}$  or  $\text{Cl}^-$  at similar concentrations and characterised the surface and cross-sectional morphologies of the  $\text{Cu}_2\text{S}$  formed. The primary aim of this work was to determine how the structure and properties of the  $\text{Cu}_2\text{S}$  films changed with the type of anion present and to shed light on the impact of groundwater anions on the corrosion of nuclear waste containers under Swedish/Finnish/Canadian DGR conditions.

## 2 | EXPERIMENTAL METHODS

### 2.1 | Sample preparation

The material studied was P-doped (30–100 wt. ppm), O-free Cu (<5 wt. ppm O, Cu-OFP), provided by the Swedish Nuclear Fuel and Waste Management Company (SKB). Cu disk working electrodes (1 cm in diameter) were cut from the copper block and connected to a stainless-steel shaft. The connection was painted with a nonconductive epoxy to prevent the solution from contacting the Cu/steel junction during the experiments. The electrode was then heated to 60°C for 12 h to promote adhesion of the epoxy. The exposed flat Cu surface was ground successively with 240, 600, 800, 1000, and 1200 grit SiC paper and then polished to a mirror finish using 1  $\mu\text{m}$ , 0.3  $\mu\text{m}$ , and, finally, 0.05  $\mu\text{m}$   $\text{Al}_2\text{O}_3$  suspensions. Before each experiment, electrodes were washed with Type I water (resistivity = 18.2  $\text{M}\Omega\text{-cm}$ , obtained from a Thermo Scientific Barnstead Nanopure 7143 ultrapure water system), ultrasonically cleaned using reagent-grade methanol, and finally washed with Type I water, and dried using a stream of Ar.

### 2.2 | Long-term corrosion experiments

To ensure anoxic conditions, the long-term corrosion experiments were performed in an Ar-purged anaerobic

chamber (Canadian Vacuum Systems Ltd.), maintained at a positive pressure (2–4 mbar), using an MBraun glove box control system. The  $O_2$  content in the chamber was analysed with an MBraun  $O_2$  probe with a detection limit of  $1.4 \text{ mg/m}^3$ . The anaerobic chamber was maintained at a total  $[O_2] \leq 4.2 \text{ mg/m}^3$ , which included the contribution from both  $O_2$  and water vapour residues. Using Henry's law, the  $[O_2]$  dissolved in the solution was calculated to be  $\leq 1.3 \times 10^{-9} \text{ M}$ . The actual  $[O_2]$  in any solution in the chamber would be less than this value. Despite the possibility of minor traces of  $O_2$  being present, it is unlikely that copper oxides played any role, since  $Cu_2S$  is more stable in  $SH^-$  solution than  $Cu_2O$ , based on thermodynamic data for the conversion from  $Cu_2O$  to  $Cu_2S$  in  $SH^-$  solutions:  $Cu_2O (s) + SH^- (aq) \rightarrow Cu_2S (s) + OH^- (aq)$ ,  $\Delta G^\circ = -101.46 \text{ kJ/mol}$  at  $298 \text{ K}$ <sup>[28]</sup>; and from the available literature.<sup>[29–32]</sup>

The solutions used were anoxic  $0.1 \text{ M Cl}^-$ , or  $0.1 \text{ M}$  or  $0.5 \text{ M SO}_4^{2-}$  solutions containing different  $[SH^-]$  ( $5 \times 10^{-5} \text{ M}$ ,  $5 \times 10^{-4} \text{ M}$ , and  $1 \times 10^{-3} \text{ M}$ ). These solutions were prepared with reagent-grade sodium sulphide ( $Na_2S \cdot 9H_2O$ , 98.0% assay, purchased from Sigma-Aldrich), sodium chloride ( $NaCl$ , 99.0% assay, purchased from Fisher Chemical), sodium sulphate ( $Na_2SO_4$ , 99.0% assay, purchased from Fisher Chemical) and Type I water. The electrolyte volume was 1 L.

Electrodes were immersed in the anoxic  $SH^-$  solutions for various exposure periods at room temperature,  $25 \pm 2^\circ\text{C}$ . A conventional three-electrode cell was employed, with the Cu electrode as the working electrode, a Pt plate as the counter electrode, and a saturated calomel reference electrode (SCE). Before each experiment, electrodes were cathodically cleaned at  $-1.5 \text{ V/SCE}$  for 1 min and then at  $-1.15 \text{ V/SCE}$  for 1 min to reduce the air-formed oxides during sample preparation. The corrosion potential ( $E_{CORR}$ ) was monitored, and electrochemical impedance spectroscopy (EIS) measurements were performed intermittently over the full exposure periods. The EIS measurements were carried out over the frequency range from  $10^5$  to  $10^{-3} \text{ Hz}$  using a Solarton 1287 electrochemical interface and a Solarton 1255B frequency response analyser at an ac potential amplitude of  $10 \text{ mV}$ . The validity of the impedance spectra was checked using the Kramers–Krönig transform.

Since the exposure periods were long, the  $[SH^-]$  was monitored weekly by measuring the pH. If  $SH^-$  depletion had occurred, as indicated by a decrease in pH (since the formation of copper sulphide clusters would release protons<sup>[33]</sup>),  $SH^-$  was replenished to the initial concentration as described previously.<sup>[13]</sup>

## 2.3 | Analyses of the $Cu_2S$ films

Once removed from the solution, Cu electrodes were rinsed with Type I water for 1 min and dried with Ar gas. Analyses were then performed after a minimum period of interim storage in the anaerobic chamber ( $<30 \text{ min}$ ). The surface and cross-sectional morphologies of these corroded Cu electrodes were observed using a Leo 1540 scanning electron microscope (SEM) equipped with a focussed ion beam (FIB) (Zeiss Nano Technology Systems Division). The composition of the films formed on the surface of these Cu electrodes was qualitatively analysed by energy dispersive X-ray spectroscopy (EDS) using a Leo 1540 FIB/SEM microscope (with an O detection limit of 1 at.%).

## 3 | RESULTS AND DISCUSSION

### 3.1 | $E_{CORR}$ measurements

The evolution of the  $E_{CORR}$  in anoxic  $0.1 \text{ M Cl}^-$ -containing solutions containing different  $[SH^-]$  ranging from  $5 \times 10^{-5} \text{ M}$  to  $1 \times 10^{-3} \text{ M}$  as a function of immersion time is shown in Figure 1a. On switching to an open circuit, the potential rose rapidly from the applied cathodic cleaning value (i.e.,  $\leq 12 \text{ min}$ ). Generally, the value of  $E_{CORR}$  then established was more negative at a higher  $[SH^-]$ . All  $E_{CORR}$  values exhibited positive shifts with the consumption of  $SH^-$ , due to the deposition of  $Cu_2S$  on the Cu surface as corrosion proceeded.  $SH^-$  depletion was particularly rapid at the lowest  $[SH^-]$  (i.e.,  $5 \times 10^{-5} \text{ M}$ ), as indicated by the significant decrease in pH, Figure 1a. When the  $SH^-$  was replenished,  $E_{CORR}$  decreased to the original value of  $\sim -0.82 \text{ V/SCE}$ , indicating a competition between  $SH^-$  and  $Cl^-$  for surface adsorption sites.<sup>[20]</sup> At high  $[SH^-]$  (i.e.,  $\geq 5 \times 10^{-4} \text{ M}$ ),  $E_{CORR}$  slowly increased to a slightly more positive value over an extended exposure time, indicating that minimal  $SH^-$  depletion occurred, suggesting that the structure and properties of the  $Cu_2S$  films may be different from those formed at the low  $[SH^-]$ , since their structure and properties are highly dependent on the sulphide concentration, sulphide flux and the chloride to sulphide concentration ratio.<sup>[17]</sup>

$E_{CORR}$ -time plots recorded in  $SO_4^{2-}$ -containing solutions over the same  $[SH^-]$  range are shown in Figure 1b. At low  $[SH^-]$ , the solution pH did not decrease, nor was there a positive shift of  $E_{CORR}$ , meaning that there was no depletion of the bulk  $[SH^-]$ . This suggested that there is a lower  $SH^-$  consumption rate, and hence a lower  $Cu_2S$  film growth rate, than in  $Cl^-$ -containing solution, indicating differences in the influences of  $SO_4^{2-}$  and

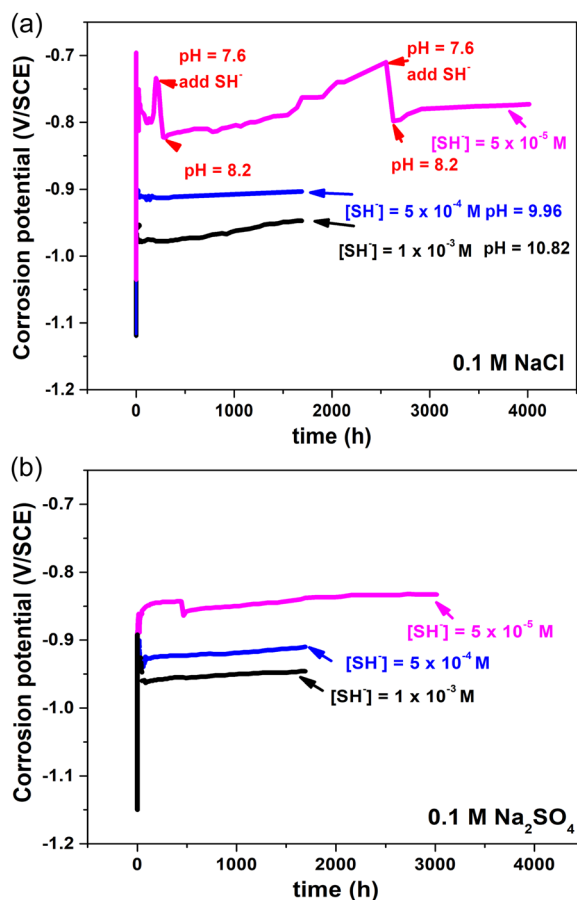


**FIGURE 1** The corrosion potentials of P-doped O-free Cu as a function of immersion time in: (a) anoxic 0.1 M Cl<sup>-</sup>-containing solution containing different [SH<sup>-</sup>] (from references<sup>[13,14,20]</sup>); and (b) anoxic 0.1 M SO<sub>4</sub><sup>2-</sup>-containing solution containing the same [SH<sup>-</sup>]. [Color figure can be viewed at [wileyonlinelibrary.com](http://wileyonlinelibrary.com)]

Cl<sup>-</sup> on the Cu surface.<sup>[20]</sup> The strong co-adsorption of SO<sub>4</sub><sup>2-</sup> and H<sub>2</sub>O indicated in electrochemical experiments<sup>[26]</sup> may inhibit the initial SH<sup>-</sup> adsorption step required to initiate Cu<sub>2</sub>S formation. At high [SH<sup>-</sup>], the  $E_{CORR}$  responses were similar to those observed in Cl<sup>-</sup>-containing solution, suggesting a similar film growth process.

### 3.2 | EIS measurements

EIS measurements were conducted over the exposure periods shown in Figure 1 to characterise the corrosion (film growth) process occurring. Figure 2 shows EIS spectra (in the form of Bode plots) recorded as a function of immersion time in an anoxic 0.1 M SO<sub>4</sub><sup>2-</sup> + 5 × 10<sup>-5</sup> M SH<sup>-</sup> solution. As previously observed in anoxic 0.1 M Cl<sup>-</sup> + 5 × 10<sup>-5</sup> M SH<sup>-</sup> solutions,<sup>[14]</sup> the spectra exhibited two poorly-defined capacitive loops, identified by the red and blue arrows in Figure 2b. In the study in Cl<sup>-</sup>-

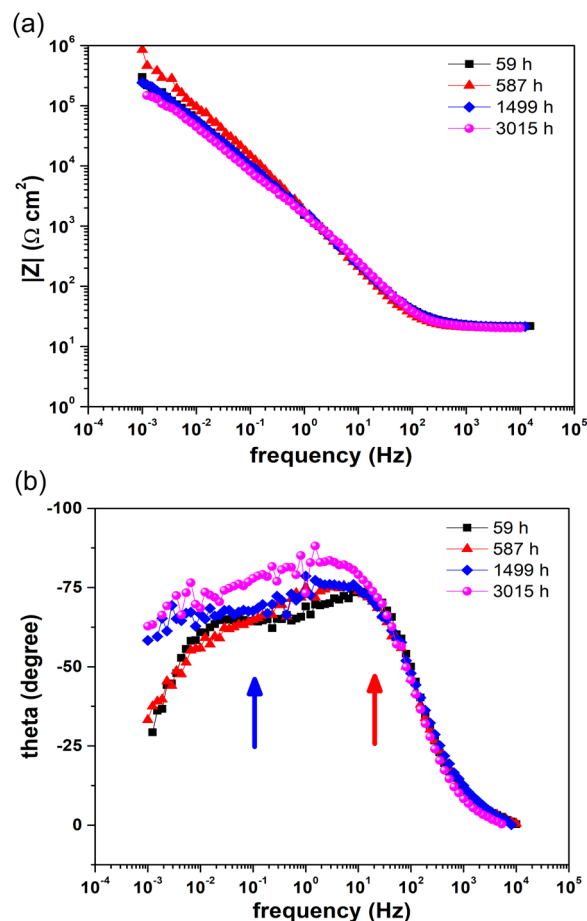


**FIGURE 2** Electrochemical impedance spectroscopic (EIS) spectra (in the form of Bode plots, [a] and [b]) recorded on P-doped O-free Cu after immersion in an anoxic 5 × 10<sup>-5</sup> M SH<sup>-</sup> + 0.1 M SO<sub>4</sub><sup>2-</sup> solution for different exposure times. [Color figure can be viewed at [wileyonlinelibrary.com](http://wileyonlinelibrary.com)]

containing solutions, the response at high frequencies (marked by the red arrow) was attributed to the interfacial charge transfer process involving the creation of the Cu<sup>I</sup> species at the Cu surface and the associated double layer capacitance distributed across the whole surface, either exposed metal or Cu<sub>2</sub>S since Cu<sub>2</sub>S is electrically conducting.<sup>[13,14]</sup> The Cu<sup>I</sup> species was stabilised by complexation with adsorbed SH<sup>-</sup>, and this complex is the precursor to the formation of the Cu<sub>2</sub>S film. The lower-frequency response was attributed to the formation of an adsorbed surface layer.

The linear increase in log|Z| (the logarithm of the impedance modulus) at frequencies ≤ 10<sup>-1</sup> Hz (Figure 2a) and the increase in phase angle (theta) to a value in the range 45°–60° (Figure 2b) indicate a significant contribution to the control of the film growth process by SH<sup>-</sup> diffusion, both within the growing Cu<sub>2</sub>S film and in the bulk of the solution, as was also observed in the Cl<sup>-</sup>-containing solution.<sup>[14]</sup> The impedance response in the

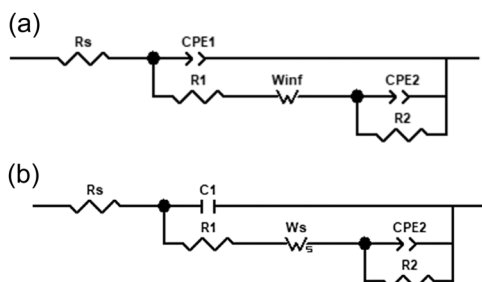


**FIGURE 3** The electrical equivalent circuits used to fit the experimentally acquired electrochemical impedance spectroscopic (EIS) spectra: (a) in anoxic  $5 \times 10^{-5}$  M  $\text{SH}^-$  solution; and (b) in anoxic  $\geq 5 \times 10^{-4}$  M  $\text{SH}^-$  solutions.

high-frequency range (Figure 2b, red arrow) showed only a small change in position on the frequency scale with exposure time, indicating only a minor modification of the interfacial impedance response as the  $\text{Cu}_2\text{S}$  film accumulated on the surface, as previously observed in the  $\text{Cl}^-$ -containing solution.<sup>[14]</sup>

The electrical equivalent circuit (Figure 3a) proposed previously<sup>[14]</sup> was used to fit these spectra. In this circuit,  $R_s$  represents the solution resistance,  $\text{CPE}_1$  is a constant phase element (CPE) representing the double-layer capacitance across the  $\text{Cu}_2\text{S}$ /electrolyte interface,  $R_1$  is the charge transfer resistance for the formation of  $\text{Cu}(\text{SH})_{\text{ads}}$  species at the  $\text{Cu}$ /electrolyte interface,  $\text{CPE}_2$  and  $R_2$  are the capacitance and resistance of the adsorbed surface layer, respectively, and  $W_{\text{inf}}$  is an infinite Warburg element attributed to the  $\text{SH}^-$  diffusion in solution. These fits yielded values of the overall interfacial polarisation resistance ( $R_p$ ),

$$R_p = R_1 + R_2,$$

with  $R_p^{-1}$  proportional to the film growth rate (which can be considered as directly proportional to the corrosion rate). The change of the polarisation resistance is plotted as a function of exposure period for both  $\text{SO}_4^{2-}$ - and  $\text{Cl}^-$ -containing solutions in Figure 4. Over the first  $\sim 300$  h of exposure, the  $R_p$  values in  $\text{Cl}^-$ -containing solutions were smaller than those in  $\text{SO}_4^{2-}$ -containing solutions, suggesting a faster film growth rate. This would cause faster  $\text{SH}^-$  consumption, leading to its depletion, consistent with the  $E_{\text{CORR}}$  and pH measurements in Figure 1. With the increase of immersion time up to 1500 h, the  $R_p$  values in both solutions increased slightly (by approximately a factor of 2) as film deposition occurred. At longer exposure times of 2500 h,  $\text{SH}^-$  was replenished in  $\text{Cl}^-$ -containing solutions, leading to the decrease of  $R_p$  values. However, in  $\text{SO}_4^{2-}$ -containing solution,  $R_p$  values continued to increase. Since our

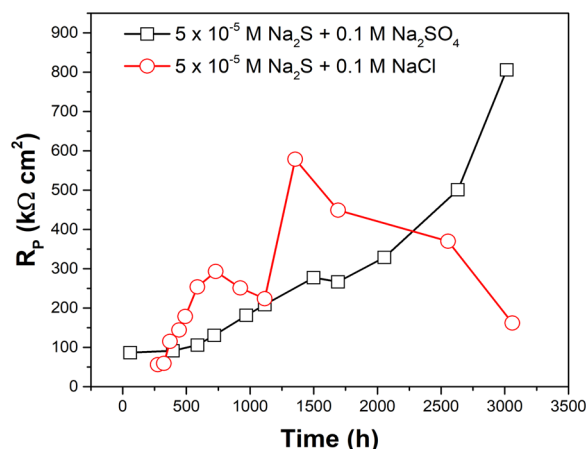


**FIGURE 4** The polarisation resistance obtained from the electrochemical impedance spectroscopic (EIS) spectra recorded as a function of immersion time in anoxic  $\text{SO}_4^{2-}$  (Figure 2a) and in  $\text{Cl}^-$ -containing<sup>[14]</sup> solutions. [Color figure can be viewed at [wileyonlinelibrary.com](http://wileyonlinelibrary.com)]

previous study demonstrated that the film growth was proceeding under diffusion control in  $\text{Cl}^-$ -containing solutions,<sup>[14]</sup> and that film deposition occurred at the  $\text{Cu}_2\text{S}$ /electrolyte interface,<sup>[23]</sup> the dependence of film growth rate on  $\text{SH}^-$  supply is consistent with a porous film which does not act as a significant corrosion barrier as it thickens.

When  $[\text{SH}^-]$  was increased to  $5 \times 10^{-4}$  M, two time constants similar to, but better defined than those observed at the lower  $[\text{SH}^-]$ , were observed, as shown in Figure 5a,b. This behaviour was similar to that observed previously in  $\text{Cl}^-$ -containing solutions with the same  $[\text{SH}^-]$ ,<sup>[13]</sup> and shows that the overall film growth process proceeded by a mechanism similar to that observed at the lower  $[\text{SH}^-]$ , but with a number of observable differences. The location of the two time constants on the frequency axis shifted to slightly lower frequencies, consistent with both a decrease in the rate of the interfacial ( $\text{Cu}/\text{Cu}_2\text{S}$ ) process (as indicated also by an increase in  $|Z|$  as the frequency decreased, Figure 5a) and a higher resistance (increased protectiveness) of the  $\text{Cu}_2\text{S}$  layer. The phase angle at the low-frequency limit was much lower, as shown in Figure 5b than that observed at  $[\text{SH}^-] = 5 \times 10^{-5}$  M, as shown in Figure 2b, indicating a significantly lower contribution of  $\text{SH}^-$  diffusion to the impedance at this higher  $[\text{SH}^-]$ . Comparison to previously recorded spectra over a similar exposure period showed that at short exposure times (i.e.,  $\leq 100$  h), the phase angle recorded in  $\text{Cl}^-$ -containing solution approached zero at  $10^{-3}$  Hz, indicating a minimal contribution of  $\text{SH}^-$  diffusion to the early stages of film formation. As the exposure time increased (up to 1691 h)

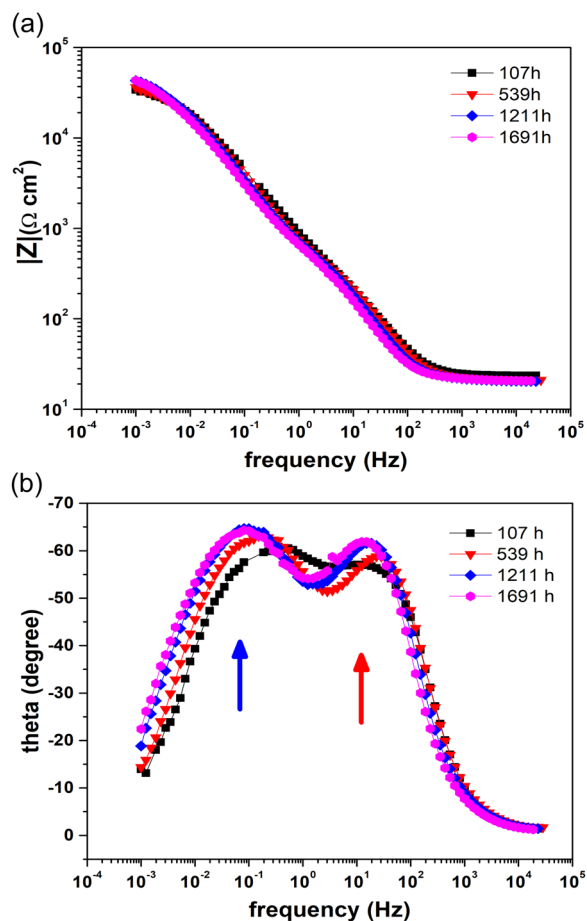


**FIGURE 5** Electrochemical impedance spectroscopic (EIS) spectra (in the form of Bode plots, [a] and [b]) recorded on P-doped O-free Cu after immersion in anoxic  $5 \times 10^{-4}$  M  $\text{SH}^-$  + 0.1 M  $\text{SO}_4^{2-}$  solution for different exposure times. [Color figure can be viewed at [wileyonlinelibrary.com](#)]

in  $\text{Cl}^-$ -containing solution, the phase angle increased to values approaching  $15^\circ$ – $20^\circ$ <sup>[13]</sup> indicating an increasing contribution to the impedance from  $\text{SH}^-$  diffusion as the  $\text{Cu}_2\text{S}$  film accumulated. This difference in phase angle response indicated a more significant effect of  $\text{SH}^-$  diffusion on the film growth process in  $\text{SO}_4^{2-}$ -containing, compared to  $\text{Cl}^-$ -containing, solutions.

When the  $[\text{SH}^-]$  was  $\geq 5 \times 10^{-4}$  M, the change in film structure from porous to compact required a change in the electrical equivalent circuit (Figure 3b) required to fit the EIS spectra in Figure 5 as previously used.<sup>[13]</sup> In this circuit,  $R_s$  represents the solution resistance,  $C_1$  is the double-layer capacitance across the  $\text{Cu}_2\text{S}$ /electrolyte interface since the sulphide film is electrically conducting,  $R_1$  is the charge-transfer resistance for the formation of Cu(I) species at the Cu/ $\text{Cu}_2\text{S}$  interface,  $\text{CPE}_2$  and  $R_2$  are the capacitance and resistance of the adsorbed surface layer, respectively, and  $W_s$  is a short Warburg

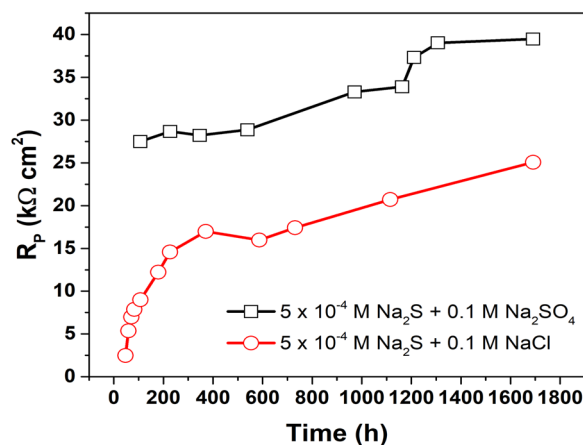


**FIGURE 6** The polarisation resistance obtained from electrochemical impedance spectroscopic (EIS) spectra recorded in anoxic  $\text{SO}_4^{2-}$ - (Figure 4a) and  $\text{Cl}^-$ -containing solutions<sup>[13]</sup> as a function of immersion time. [Color figure can be viewed at [wileyonlinelibrary.com](#)]

element attributed to a diffusion process of  $\text{Cu}^+$  through the sulphide film. The sum of  $R_1$  and  $R_2$  would yield the value of the polarisation resistance,  $R_p$ . Figure 6 shows the  $R_p$  values obtained in  $\text{SO}_4^{2-}$ - and  $\text{Cl}^-$ -containing solutions obtained from EIS fitting (Figure 5a and Chen et al.<sup>[13]</sup>) plotted as a function of exposure time. The values of  $|Z|$  were between 1 and 2 orders of magnitude lower than those recorded at the lower  $[\text{SH}^-]$  ( $5 \times 10^{-5}$  M) in both  $\text{Cl}^-$ - and  $\text{SO}_4^{2-}$ -containing solutions. This difference provides a measure of the major influence of diffusive transport in determining the rate of film growth at the lower  $[\text{SH}^-]$ . The  $R_p$  values at short exposure times ( $\leq 200$  h) show film growth was more rapid (i.e.,  $R_p$  was lower) in  $\text{Cl}^-$ -containing than  $\text{SO}_4^{2-}$ -containing solutions, but with exposure time in  $\text{Cl}^-$ -containing solutions, decreased to a value just slightly less than that in  $\text{SO}_4^{2-}$ -containing solution. Based on the differences in the values of the phase angle at the low-frequency limit, this appears attributable mainly to a much more significant contribution of  $\text{SH}^-$  diffusion in the films present on Cu in  $\text{Cl}^-$ -containing solutions than in  $\text{SO}_4^{2-}$ -containing solutions, suggesting that the film present in  $\text{Cl}^-$ -containing solution was initially significantly less of a barrier to  $\text{SH}^-$  transport. This is consistent with electrochemical results recorded under transport-controlled conditions in which lower anodic limiting currents were recorded in  $\text{SO}_4^{2-}$ -containing solutions than in  $\text{Cl}^-$ -containing solutions.<sup>[26]</sup> At longer exposure times ( $> 500$  h), the film growth rate remained slightly lower in the  $\text{SO}_4^{2-}$ -containing solution ( $R_p$  was slightly higher), suggesting a slightly, but not significantly, lower barrier for  $\text{SH}^-$  diffusion to the corroding Cu surface.

EIS spectra were obtained in both  $\text{Cl}^-$ - and  $\text{SO}_4^{2-}$ -containing solutions when  $[\text{SH}^-]$  was further increased to  $10^{-3}$  M, Figures 7 and 8. At lower  $[\text{SH}^-]$ , the same two time constants were observed. In the  $\text{Cl}^-$ -containing solution, only the high-frequency time constant was initially observed. This time constant remained visible in the spectra as the low-frequency time constant developed, confirming that the interfacial impedance response remained detectable despite the accumulation of the  $\text{Cu}_2\text{S}$  deposit. At very short exposure times (up to 21 h), the phase angle at the low-frequency limit approached zero, indicating minimal control of the film growth process by  $\text{SH}^-$  diffusion. At intermediate exposure times (up to 83 h), the phase angle at  $10^{-3}$  Hz was markedly higher, indicating an increased control of film growth by  $\text{SH}^-$  transport in the accumulating deposit. At the longest exposure periods ( $>167$  h), the phase angle approached  $\sim 60^\circ$  (Figure 7b), indicating that the film was becoming a substantial barrier to corrosion.

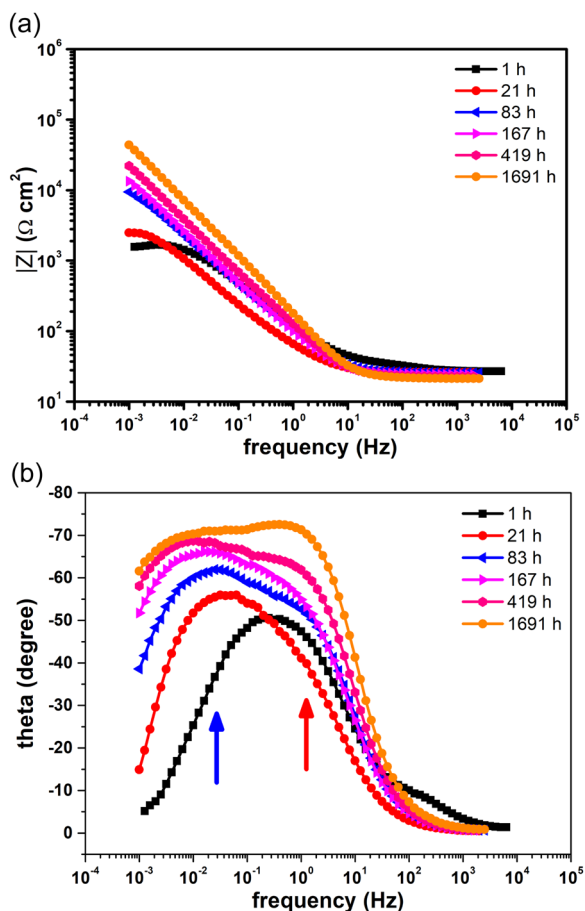


**FIGURE 7** Electrochemical impedance spectroscopic (EIS) spectra (in the form of Bode plots, [a] and [b]) recorded on P-doped oxygen-free Cu after immersion in anoxic  $1 \times 10^{-3}$  M  $\text{SH}^-$  + 0.1 M  $\text{Cl}^-$  solution for different exposure times. [Color figure can be viewed at [wileyonlinelibrary.com](#)]

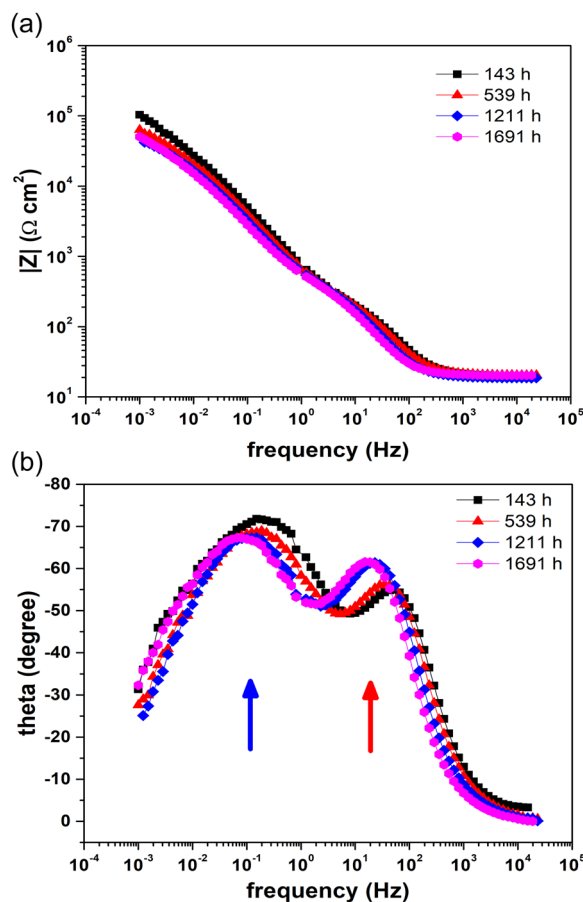


**FIGURE 8** Electrochemical impedance spectroscopic (EIS) spectra (in the form of Bode plots, [a] and [b]) recorded on P-doped oxygen-free Cu after immersion in anoxic  $1 \times 10^{-3}$  M  $\text{SH}^-$  + 0.1 M  $\text{SO}_4^{2-}$  solution for different exposure times. [Color figure can be viewed at [wileyonlinelibrary.com](#)]

In  $\text{SO}_4^{2-}$ -containing solution, the impedance spectra were very similar to those recorded at the lower  $[\text{SH}^-]$  of  $5 \times 10^{-4}$  M and did not change significantly as the exposure time increased.

Figure 9 shows that the values of  $R_p$  as a function of immersion time were very different in  $\text{Cl}^-$ - and  $\text{SO}_4^{2-}$ -containing solutions at short exposure periods but effectively the same beyond an exposure period of  $\sim 1000$  h. At short exposure periods, the film growth rate in  $\text{Cl}^-$ -containing solutions was considerably higher than in  $\text{SO}_4^{2-}$ -containing solutions, as observed at the lower  $[\text{SH}^-]$  of  $5 \times 10^{-4}$  M. It confirms that, in the absence of an accumulation of  $\text{Cu}_2\text{S}$ , the film growth rate is high in  $\text{Cl}^-$ -containing solution, as observed electrochemically in anodic polarisation experiments. These observations suggest  $\text{Cl}^-$  may have initially accelerated corrosion, possibly by facilitating dissolution as  $\text{CuCl}_2^-$  before its conversion to  $\text{Cu}_2\text{S}$ .<sup>[14]</sup> However, once  $\text{Cu}_2\text{S}$  film formation commenced, the corrosion rate decreased as the film

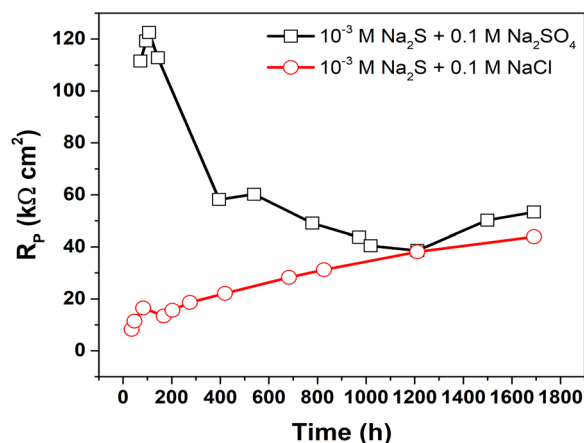


**FIGURE 9** The polarisation resistance from electrochemical impedance spectroscopic (EIS) spectra recorded in anoxic  $1 \times 10^{-3}$  M  $\text{SH}^- + 0.1$  M  $\text{SO}_4^{2-}$  and  $1 \times 10^{-3}$  M  $\text{SH}^- + 0.1$  M  $\text{Cl}^-$  solutions as a function of immersion time. [Color figure can be viewed at [wileyonlinelibrary.com](http://wileyonlinelibrary.com)]

accumulated. By contrast,  $\text{SO}_4^{2-}$  initially inhibited  $\text{Cu}_2\text{S}$  formation, as observed electrochemically, with the corrosion rate increasing slightly with exposure time. The coincidence in the film growth rates at longer times demonstrated that, for sufficient film coverage, the corrosion process became dominated by the properties of the film, with any influence of the kinetics at the Cu/ $\text{Cu}_2\text{S}$  interface obscured. This contrasted with the observations at the lower  $[\text{SH}^-]$  of  $5 \times 10^{-5}$  M, when the difference in film growth rate at long times, Figure 4, remained sensitive to the nature of the anion. For the two higher  $[\text{SH}^-]$  the differences in film growth rate at longer exposure times were marginal, suggesting that there was little difference in the ability of the  $\text{Cu}_2\text{S}$  films present to control the interfacial corrosion rate by transport of species through the sulphide film. This could indicate that the transport of  $\text{Cu}^+$  species through the sulphide film, to be incorporated into the film at the  $\text{Cu}_2\text{S}/$  electrolyte interface, limits the overall rate at these high  $[\text{SH}^-]$  due to the structure and properties of the deposited sulphide film.

### 3.3 | Surface and cross-sectional morphologies of films grown at a low ionic strength

Figure 10a,b shows SEM micrographs of the surface and a FIB-cut cross section of a specimen corroded for 3015 h in a 0.1 M  $\text{SO}_4^{2-}$ -containing solution containing  $5 \times 10^{-5}$  M  $\text{SH}^-$ . The deposit comprised a mixture of small crystals and agglomerated small particulates apparently less than  $\sim 100$  nm in dimension, with the

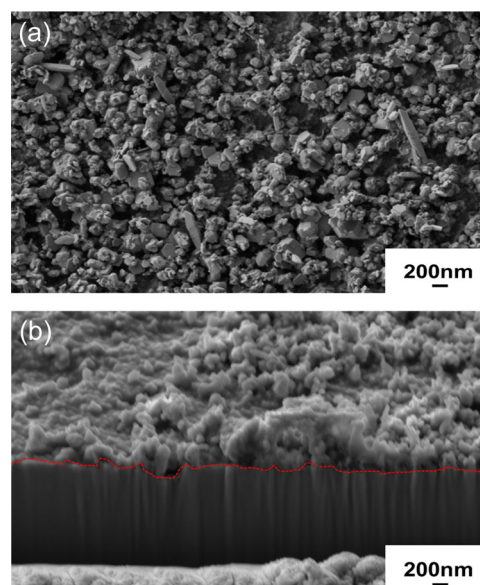


**FIGURE 10** Scanning electron microscope surface (a) and cross-sectional (b) images of P-doped O-free Cu after 3015 h immersion in anoxic  $5 \times 10^{-5}$  M  $\text{SH}^- + 0.1$  M  $\text{SO}_4^{2-}$  solution. The red dashed line shows the interface of  $\text{Cu}_2\text{S}$  film and Cu matrix. [Color figure can be viewed at [wileyonlinelibrary.com](http://wileyonlinelibrary.com)]

cross section demonstrating that the film was porous and non-protective. While the Cu/ $\text{Cu}_2\text{S}$  interface was slightly roughened, there was no evidence of any locally penetrated sites, confirming that corrosion had progressed generally uniformly across the surface and that a significant area of the Cu substrate remained exposed to the solution. A similar crystalline/nanoparticulate deposit was observed after corrosion in a 0.1 M  $\text{Cl}^-$ -containing solution containing the same  $[\text{SH}^-]$ ,<sup>[14]</sup> although the  $\text{Cu}_2\text{S}$  film was less uniformly distributed and visibly more porous.

These observations are consistent with the impedance analyses (Figures 2 and 4) and our previous results obtained in 0.1 M  $\text{Cl}^-$ -containing solution containing  $5 \times 10^{-5}$  M  $\text{SH}^-$  which demonstrated film growth controlled by  $\text{SH}^-$  diffusion,<sup>[14]</sup> with the process occurring slightly faster at longer exposure times in the  $\text{Cl}^-$ -containing solution. Diffusion-controlled film growth was demonstrated at this  $[\text{SH}^-]$  in  $\text{Cl}^-$ -containing solution by the observation of a linear film growth law (based on measured film thicknesses<sup>[14]</sup>). The mixture of crystals and nanoscale particles within the film was to be expected, since it has been demonstrated that  $\text{Cu}^+$  transport from the corroding surface occurs via a combination of ionic complexes ( $\text{Cu}(\text{SH})_2^-$ ) and  $\text{Cu}_3\text{S}_3$  clusters.<sup>[18,19]</sup> The agglomeration of clusters was to be expected in the solutions used in this study, which had significant ionic strengths (see section 3.4 below).



When the  $[\text{SH}^-]$  was increased to  $5 \times 10^{-4}$  M, the  $\text{Cu}_2\text{S}$  deposit was much thicker, consistent with the increased flux of  $\text{SH}^-$ , and more crystalline than observed at the lower  $[\text{SH}^-]$ , Figure 11a,b. Inspection of the  $\text{Cu}/\text{Cu}_2\text{S}$  interface showed no evidence of localised penetrations. A similar more crystalline and dense film was also observed after growth for a similar exposure period in  $\text{Cl}^-$ -containing solution,<sup>[13]</sup> although the surface morphology of the films was different, indicating an influence of the anions on the  $\text{Cu}_2\text{S}$  deposition process. Additionally, in  $\text{Cl}^-$ -containing solution, the microgalvanic coupling could have led to nonuniform film growth and localised penetrations when  $[\text{SH}^-]$  was increased to this concentration.<sup>[18]</sup>

Close inspection of the surfaces of the deposited crystals, Figure 11a, shows they were decorated with a fine particulate layer. Such a layer was much more obvious on the surface of  $\text{Cu}_2\text{S}$  crystals grown in  $\text{Cl}^-$ -containing solutions.<sup>[18]</sup> Since these large crystals grew by the incorporation of  $\text{Cu}(\text{SH})_2^-/\text{Cu}_3\text{S}_3$  species transported from the corroding surface, this difference suggests that the incorporation of  $\text{Cu}_3\text{S}_3$  species may be hindered more by the adsorption of  $\text{Cl}^-$  than  $\text{SO}_4^{2-}$  ions at the  $\text{Cu}_2\text{S}$  surfaces.

This could partially account for the apparently more extensive film growth observed in  $\text{SO}_4^{2-}$ -containing solutions, based on film thickness measurements, shown in Figure 12, despite the evidence from the impedance measurements that the corrosion rate was slightly lower in the presence of  $\text{SO}_4^{2-}$  as shown in Figure 6. In the presence of either of the two anions, the film growth rate

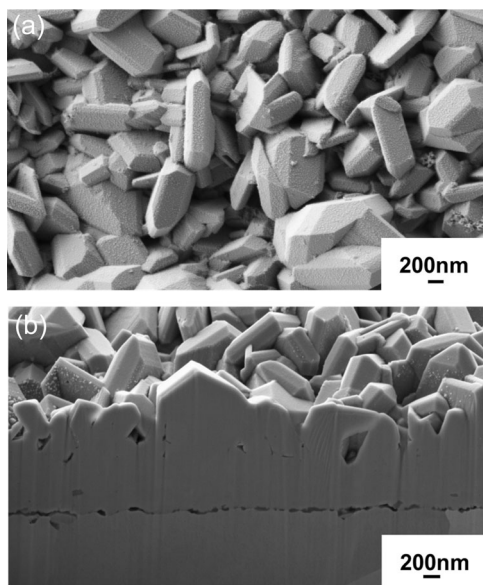


**FIGURE 11** Scanning electron microscope surface (a) and cross-sectional (b) images of P-doped O-free Cu after 1691 h immersion in an anoxic  $5 \times 10^{-4}$  M  $\text{SH}^- + 0.1$  M  $\text{SO}_4^{2-}$  solution.

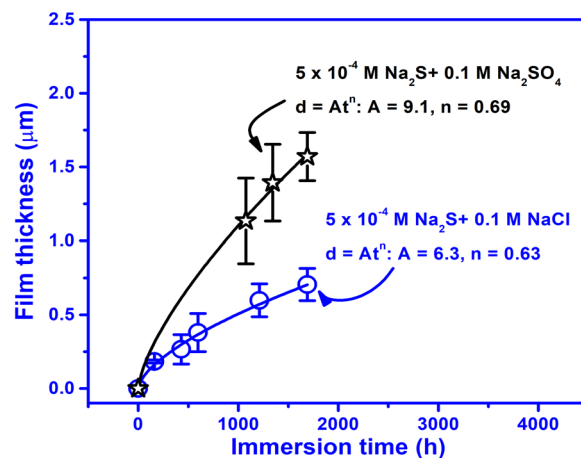


**FIGURE 12** Growth laws and average thicknesses of the  $\text{Cu}_2\text{S}$  films formed on P-doped O-free Cu after exposure to anoxic  $\text{SH}^-$  solutions containing different  $[\text{SO}_4^{2-}]$  or  $[\text{Cl}^-]$  as a function of immersion time. The blue plot is cited from Chen et al.<sup>[13]</sup> to compare the growth of the  $\text{Cu}_2\text{S}$  film in  $\text{SO}_4^{2-}$ -containing solution. [Color figure can be viewed at [wileyonlinelibrary.com](http://wileyonlinelibrary.com)]

(based on film thickness) exhibited a logarithmic law, indicating the formation of a more compact and protective film than observed at  $5 \times 10^{-5}$  M  $\text{SH}^-$ . This possible explanation is supported by the analytical detection of Cu in  $\text{Cl}^-$ -containing solutions, which would suggest the transport of some clusters into the solution. If this was the case, the film thickness measurement would have underestimated the corrosion rate.

At the highest  $[\text{SH}^-]$  employed in this study ( $10^{-3}$  M), the EIS data, shown in Figure 9, showed that, despite significant differences in the film growth rate at short exposure times, the rates beyond  $\sim 100$  h were effectively the same, suggesting that film growth was dominated by the transport of  $\text{Cu}^I$  through  $\text{Cu}_2\text{S}$  deposits with similar properties, leading to a uniform, predominantly crystalline deposit. Again, an inspection of the  $\text{Cu}/\text{Cu}_2\text{S}$  interface showed no evidence of localised penetrations as shown in Figure 13.

By contrast, after a similar exposure period the film deposited in a  $\text{Cl}^-$ -containing solution containing the same  $[\text{SH}^-]$  showed areas only sparsely covered by a deposit adjacent to areas covered by very large crystals, indicating a nonuniform deposition process. Such a situation has been shown to lead to localised penetrations that can be attributed to micro-galvanic coupling of sparsely covered, net anodic areas to densely covered, and net cathodic areas at which  $\text{Cu}(\text{SH})_2^-/\text{Cu}_3\text{S}_3$  deposition occurs, a process which can lead to localised penetrations of the Cu substrate.<sup>[20]</sup> A more thorough study would be required to determine whether such a process was avoided in  $\text{SO}_4^{2-}$ -containing solutions.

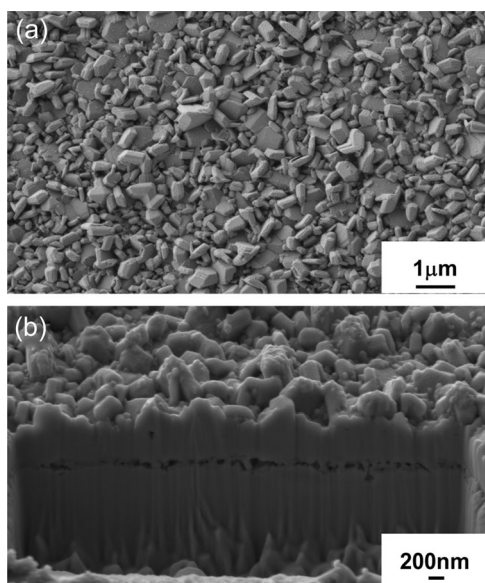


**FIGURE 13** Scanning electron microscope surface (a) and cross-sectional (b) morphologies of P-doped oxygen-free Cu after 1691 h immersion in anoxic  $1 \times 10^{-3}$  M  $\text{SH}^-$  +  $0.1$  M  $\text{SO}_4^{2-}$  solution.

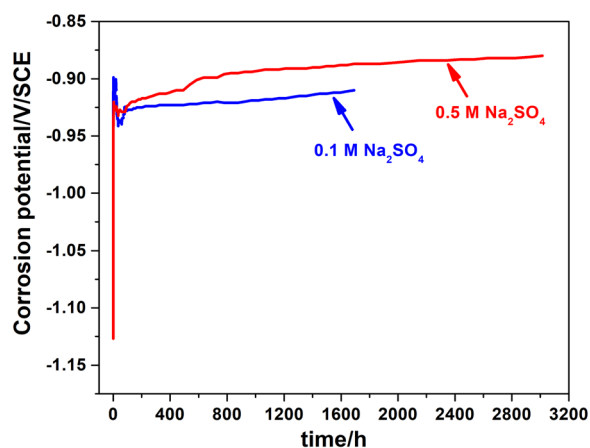


**FIGURE 14** The corrosion potentials recorded on P-doped O-free Cu as a function of immersion time in anoxic  $5 \times 10^{-4}$  M  $\text{SH}^-$  solutions containing different  $[\text{SO}_4^{2-}]$ . [Color figure can be viewed at [wileyonlinelibrary.com](http://wileyonlinelibrary.com)]

The corrosion rate data suggest micro-galvanic coupling may be confined to  $\text{Cl}^-$ -containing solutions in which the initial corrosion rates, when only minor amounts of  $\text{Cu}_2\text{S}$  have been deposited, are much higher than in  $\text{SO}_4^{2-}$ -containing solution. This higher corrosion rate in  $\text{Cl}^-$ -containing solutions would facilitate the formation of more copper sulphide clusters and complexes, and thus would accelerate the growth of the deposited  $\text{Cu}_2\text{S}$  crystals, leading to their non-uniform distribution on the Cu surface<sup>[20]</sup> (Figure 14).

### 3.4 | The influence of high ionic strength on film morphology

The above results, and those in  $\text{Cl}^-$ -containing solutions published previously,<sup>[13–20]</sup> show that the nature of the anion had an influence on both the morphology and porosity of the deposited  $\text{Cu}_2\text{S}$  layer. To investigate this influence further, a long-term corrosion experiment was performed in a solution containing  $[\text{SH}^-] = 5 \times 10^{-4}$  M with a  $[\text{SO}_4^{2-}]$  increased to  $0.5$  M. The evolution of  $E_{\text{CORR}}$  with exposure time in this solution exhibited a larger shift to more positive values (than that in  $[\text{SO}_4^{2-}] = 0.1$  M [from Figure 1]), which may reflect a slight increase in film growth rate at the higher concentration, although it is not possible to verify this without impedance measurements. After 3015 h of exposure, the deposited film was composed almost exclusively of fine particulates, with only a smattering of small crystals as shown in Figure 15a.

This film morphology was radically different from that observed when the deposit was grown in a solution containing the lower concentration of  $0.1$  M, Figure 11a. The cross section in Figure 15b shows that this finely particulate outer layer obscured a sublayer of irregular crystal growth, with some areas of the Cu surface covered by thick crystals and some only by a thin layer whose morphology was difficult to discern but appeared crystalline. It was clear that, at the high ionic strength prevailing in the  $0.5$  M solution, the agglomeration of  $\text{Cu}_3\text{S}_3$  clusters limited their incorporation into growing

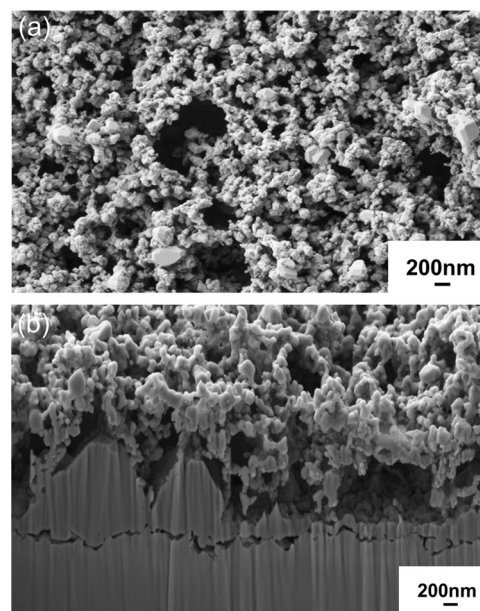


**FIGURE 15** Scanning electron microscope surface (a) and cross-sectional (b) images of P-doped O-free Cu after 3015 h immersion in an anoxic  $5 \times 10^{-4}$  M  $\text{SH}^-$  +  $0.5$  M  $\text{SO}_4^{2-}$  solution.

crystals, as observed at  $[\text{SO}_4^{2-}] = 0.1 \text{ M}$ . While the transformation of  $\text{Cu}_3\text{S}_3$  clusters into large  $\text{Cu}_2\text{S}$  crystals is not well understood, these results show that it is strongly inhibited at high ionic strength, consistent with the results obtained in concentrated  $\text{Cl}^-$ -containing solutions (i.e., 5.0 M).<sup>[20]</sup>

In a Swedish/Finnish DGR, the groundwater anions of dominant interest will be chloride and sulphate, and their expected concentrations 10 000 years after DGR closure are in the range from  $3 \times 10^{-4} \text{ M}$  to 0.154 M (chloride) and from  $2 \times 10^{-4} \text{ M}$  to  $7.2 \times 10^{-3} \text{ M}$  (sulphate), respectively.<sup>[5]</sup> In Canada, the maximum  $[\text{Cl}^-]$  in the reference crystalline rock (CR-10) and reference sedimentary rock groundwaters (SR-270) is 0.17 M and 4.74 M, respectively, with the respective maximum  $[\text{SO}_4^{2-}]$  being  $1.04 \times 10^{-2} \text{ M}$  and  $1.86 \times 10^{-2} \text{ M}$ .<sup>[33]</sup> Since  $[\text{SH}^-]$  in Swedish/Finnish/Canadian DGRs will be low (e.g.,  $[\text{SH}^-]$  in a Swedish DGR is expected to be in the range from  $10^{-7} \text{ M}$  to  $10^{-4} \text{ M}$ ,<sup>[5]</sup> and that in a Canadian DGR is not expected to exceed  $10^{-5} \text{ M}$ <sup>[34]</sup>), the sulphide film formed on the Cu container would be porous, with growth controlled by  $\text{SH}^-$  transport to the container surface from remote locations.

#### 4 | SUMMARY AND CONCLUSIONS

- The corrosion rate of Cu varied with both  $[\text{SH}^-]$  and the presence of either  $\text{Cl}^-$  or  $\text{SO}_4^{2-}$ . At low  $[\text{SH}^-]$ , the  $\text{Cu}_2\text{S}$  deposit was finely particulate in the presence of either anion. The film growth (corrosion) rates were determined by  $\text{SH}^-$  transport to the Cu surface, partially within the deposit and partially in the bulk of the solution, with long-term rates higher in  $\text{Cl}^-$ -containing solutions, suggesting that this anion maintains a more open porosity in the  $\text{Cu}_2\text{S}$  deposit than does  $\text{SO}_4^{2-}$ .
- As the  $[\text{SH}^-]$  was increased, the corrosion rate increased markedly in both  $\text{Cl}^-$ - and  $\text{SO}_4^{2-}$ -containing solution as the flux of  $\text{SH}^-$  to the corroding surface increased. At short exposure times, before the significant accumulation of a surface deposit, the corrosion rate was considerably higher in  $\text{Cl}^-$ -containing solution, suggesting that the formation of  $\text{Cu}^{\text{I}}$  chloride complexes may have accelerated corrosion before  $\text{Cu}_2\text{S}$  deposition eventually suppressed it. At longer exposure times, as the deposit accumulated, the corrosion rates in both solutions converged, indicating that the  $\text{Cu}^{\text{I}}$  transport through the more compact crystalline deposit eventually became the rate-controlling step.
- The morphology of the  $\text{Cu}_2\text{S}$  deposit formed at  $[\text{SH}^-] \geq 5 \times 10^{-4} \text{ M}$  was influenced by the nature of the anion, with a less uniform deposit formed in  $\text{Cl}^-$ -containing solution. The more extensive

decoration of the surfaces of the deposit by nanoparticles in  $\text{Cl}^-$ -containing solutions than in  $\text{SO}_4^{2-}$ -containing solutions suggests that  $\text{Cl}^-$  adsorption on the  $\text{Cu}_2\text{S}$  surfaces may have inhibited the incorporation of  $\text{Cu}_3\text{S}_3$  clusters (transported from the corroding Cu surface) into the surface  $\text{Cu}_2\text{S}$  crystals and led to their release to the bulk of the solution. At high ionic strength (i.e., in 0.5 M  $\text{SO}_4^{2-}$ -containing or 5.0 M  $\text{Cl}^-$ -containing solution) agglomeration of such clusters significantly limited their incorporation into the growing crystals.

- The much higher initial corrosion rates in  $\text{Cl}^-$ -containing solutions than in  $\text{SO}_4^{2-}$ -containing solutions ( $[\text{SH}^-] \geq 5 \times 10^{-4} \text{ M}$ ) may account for the more uneven distribution of deposited crystals observed in  $\text{Cl}^-$ -containing solution. Since such uneven distributions of deposited crystals have been associated with the occurrence of localised penetration into the Cu surface due to micro-galvanic coupling, this suggests that such a coupling process was less likely in  $\text{SO}_4^{2-}$ -containing solutions.
- Since the  $[\text{SH}^-]$  is expected to be  $\leq 10^{-4} \text{ M}$  and  $\text{SO}_4^{2-}/\text{Cl}^-$  concentrations significantly higher in Swedish/Finnish/Canadian groundwaters, the copper sulphide deposits formed on waste containers in a DGR would be porous and non-protective, leading to corrosion under  $\text{SH}^-$  transport control.

#### ACKNOWLEDGEMENTS

This research was jointly funded by the Swedish Nuclear Fuel and Waste Management Company (SKB, Solna, Sweden), the Nuclear Waste Management Organization (NWMO, Toronto, Canada), and the Natural Sciences and Engineering Research Council of Canada through Alliance Grant ALLRP5611930-20. The authors would like to thank Todd Simpson (Nanofabrication Facility, Western University) for his help with SEM/FIB.

#### DATA AVAILABILITY STATEMENT

Data that support the findings of this study are available from the corresponding author upon reasonable request.

#### ORCID

Jian Chen  <https://orcid.org/0000-0003-4021-7127>

Christina Lilja  <https://orcid.org/0000-0002-4338-5874>

Peter G. Keech  <https://orcid.org/0000-0001-8435-628X>

#### REFERENCES

- [1] P. G. Keech, P. Vo, S. Ramamurthy, J. Chen, R. Jacklin, D. W. Shoesmith, *Corros. Eng. Sci. Technol.* **2014**, 49, 425.
- [2] C. H. Boyle, S. A. Meguid, *Nucl. Eng. Des.* **2015**, 293, 403.
- [3] SKB, *Long Term Safety for the Final Repository for Spent Fuel at Forsmark—Main Report of the SR-Site Project—Volume 1*. SKB

- Swedish Nuclear Fuel and Waste Management Company, Technical Report, TR-11-01, **2011**.
- [4] F. King, M. Kolar, P. Maak, *J. Nucl. Mater.* **2008**, 379, 133.
- [5] F. King, C. Lilja, K. Pedersen, P. Pitkänen, M. Vähänen, *An Update of the State-of-the-Art Report on the Corrosion of Copper Under Expected Conditions in a Deep Geologic Repository*. SKB Swedish Nuclear Fuel and Waste Management Company, Technical Report, TR-10-67, **2010**.
- [6] T. Standish, J. Chen, R. Jacklin, P. Jakupi, S. Ramamurthy, D. Zagidulin, P. Keech, D. Shoesmith, *Electrochim. Acta* **2016**, 211, 331.
- [7] D. S. Hall, M. Behazin, W. Jeffrey Binns, P. G. Keech, *Prog. Mater. Sci.* **2021**, 118, 100766.
- [8] N. Giroud, Y. Tomonaga, P. Wersin, S. Briggs, F. King, T. Vogt, N. Diomidis, *Appl. Geochem.* **2018**, 97, 270.
- [9] H. R. Müller, B. Garitte, T. Vogt, S. Köhler, T. Sakaki, H. Weber, T. Spillmann, M. Hertrich, J. K. Becker, N. Giroud, V. Cloet, N. Diomidis, T. Vietor, *Swiss J. Geosci.* **2017**, 110, 287.
- [10] J. McMurry, *Evolution of a Canadian Deep Geologic Repository: Base Scenario*. Ontario Power Generation Report, No. 06819-REP-01200-10127-R00, **2004**.
- [11] K. Pedersen, *Microbial Processes in Radioactive Waste Disposal*. SKB Swedish Nuclear Fuel and Waste Management Company, Technical Report, TR-00-04, **2000**.
- [12] M. Guo, J. Chen, T. Martino, C. Lilja, J. A. Johansson, M. Behazin, W. J. Binns, P. G. Keech, J. J. Noël, D. W. Shoesmith, *Mater. Corros.* **2021**, 72, 300.
- [13] J. Chen, Z. Qin, D. W. Shoesmith, *J. Electrochem. Soc.* **2010**, 157, C338.
- [14] J. Chen, Z. Qin, D. W. Shoesmith, *Electrochim. Acta* **2011**, 56, 7854.
- [15] J. Chen, Z. Qin, D. W. Shoesmith, *Copper Corrosion in Aqueous Sulphide Solutions Under Nuclear Waste Repository Conditions*. Scientific Basis for Nuclear Waste Management XXXV (Buenos Aires, Argentina, Oct. 2-7, 2011), MRS Proceedings 1475, **2012**.
- [16] T. Martino, R. Partovi-Nia, J. Chen, Z. Qin, D. W. Shoesmith, *Electrochim. Acta* **2014**, 127, 439.
- [17] J. Chen, Z. Qin, D. W. Shoesmith, *Corros. Eng. Sci. Technol.* **2014**, 49, 415.
- [18] J. Chen, Z. Qin, L. Wu, J. J. Noël, D. W. Shoesmith, *Corros. Sci.* **2014**, 87, 233.
- [19] T. Martino, J. Chen, Z. Qin, D. W. Shoesmith, *Corros. Eng. Sci. Technol.* **2017**, 52, 61.
- [20] J. Chen, Z. Qin, T. Martino, D. W. Shoesmith, *Corros. Eng. Sci. Technol.* **2017**, 52, 40.
- [21] J. Chen, Z. Qin, T. Martino, D. W. Shoesmith, *Corros. Sci.* **2017**, 114, 72.
- [22] J. Chen, Z. Qin, T. Martino, M. Guo, D. W. Shoesmith, *Corros. Sci.* **2018**, 131, 245.
- [23] J. Chen, Z. Qin, D. W. Shoesmith, *Innov. Corros. Mater. Sci.* **2018**, 8, 108.
- [24] T. Martino, J. Smith, J. Chen, Z. Qin, J. J. Noël, D. W. Shoesmith, *J. Electrochem. Soc.* **2019**, 166, C9.
- [25] M. Guo, J. Chen, T. Martino, M. Biesinger, J. J. Noël, D. W. Shoesmith, *J. Electrochem. Soc.* **2019**, 166, C550.
- [26] T. Martino, J. Chen, J. J. Noël, D. W. Shoesmith, *Electrochim. Acta* **2020**, 331, 135319.
- [27] M. Guo, J. Chen, C. Lilja, V. Dehnavi, M. Behazin, J. J. Noël, D. W. Shoesmith, *Electrochim. Acta* **2020**, 362, 137087.
- [28] D. D. Wagman, W. H. Evans, V. B. Parker, R. H. Schumm, I. Halow, S. M. Bailey, K. L. Churney, R. L. Nuttall, *J. Phys. Chem. Ref. Data* **1982**, 11, 181.
- [29] J. M. Smith, J. C. Wren, M. Odziemkowski, D. W. Shoesmith, *J. Electrochem. Soc.* **2007**, 154, C431.
- [30] E. Protopopoff, P. Marcus, *Corros. Sci.* **2003**, 45, 1191.
- [31] H. M. Hollmark, P. G. Keech, J. R. Vegelius, L. Werme, L. C. Duda, *Corros. Sci.* **2012**, 54, 85.
- [32] E. M. Khairy, N. A. Darwish, *Corros. Sci.* **1973**, 13, 149.
- [33] G. W. Luther III, S. M. Theberge, T. F. Rozan, D. Rickard, C. C. Rowlands, A. Oldroyd, *Environ. Sci. Technol.* **2002**, 36, 394.
- [34] M. Behazin, K. Pedersen, L. Li, L. Abrahamsen-Mills, A. Boylan, N. Bryan, *State of Science Review of Sulfide Production in Deep Geological Repositories for Used Nuclear Fuel*. NWMO Nuclear Waste Management Organization, Technical Report, NWMO-TR-2021-18, **2021**.

**How to cite this article:** J. Chen, X. Pan, T. Martino, C. Lilja, M. Behazin, W. J. Binns, P. G. Keech, J. J. Noël, D. W. Shoesmith, *Mater. Corros.* **2023**, 74, 1665–1676.  
<https://doi.org/10.1002/maco.202313766>